Endocrine (2019) 66:288–300
https://doi.org/10.1007/s12020-019-02009-5

ORIGINAL ARTICLE

Check for updates

Establishment and characterization of a new patient-derived anaplastic thyroid cancer cell line (C3948), obtained through fine-needle aspiration cytology

Ana T. Pinto[1] · Marta Pojo[1] · Joana Simões-Pereira[1,2,3] · Ruben Roque[4] · Ana Saramago[1] · Lúcia Roque[1] · Carmo Martins[1] · Saudade André[4] · José Cabeçadas[4] · Valeriano Leite[1,2,3] · Branca M. Cavaco[1]

Received: 29 April 2019 / Accepted: 6 July 2019 / Published online: 31 July 2019

Abstract

Purpose Anaplastic thyroid cancer (ATC) is among the most aggressive and unresectable tumors, presenting a bad prognosis. A better comprehension of the functional and molecular mechanisms behind the aggressiveness of this cancer, as well as new biomarkers for aggressiveness, prognosis, and response to therapy are required. However, owing to their irresectability, ATC tissue is not always accessible. Here we describe the establishment and characterization of a new patient-derived cell line, obtained from an unresectable ATC through fine-needle aspiration cytology (FNAC).

Methods The morphology, expression of epithelial and thyroid markers, cytogenetic, mutational and gene expression profiles, doubling time, and drug-resistance profile of the new cell line, designated C3948, were investigated using several methodologies: immunostaining, karyotype analysis, comparative genomic hybridization (CGH), fluorescent in situ hybridization (FISH), next-generation sequencing (NGS), Sanger sequencing, gene expression microarrays, cell counting, and IC_{50} determination.

Results Results indicate that C3948 cell line has a histological phenotype representative of original ATC cells and a completely aberrant karyotype with many chromosomal losses and gains; harbors mutated *TP53*, *STK11*, and *DIS3L2* genes; presents a gene expression profile similar to C643 ATC commercial cell line, but with some unique alterations; has a doubling time similar to C643; and the IC_{50} profile for paclitaxel, doxorubicin, and cisplatin is similar to C643, although higher for cisplatin.

Conclusions These observations are consistent with a typical ATC cell profile, supporting C3948 cell line as a novel preclinical model, and FNAC as a useful approach to better study anaplastic thyroid cancer, including testing of new anticancer therapies.

Keywords Anaplastic thyroid cancer · Tumor cell line · Fine-needle aspiration cytology · Genetic profile · Cytogenetic techniques · Molecular biology

Introduction

Anaplastic thyroid carcinoma (ATC) is a rare but highly aggressive cancer in humans, comprising one of the main causes of thyroid cancer-related deaths [1]. ATC's loco-

These authors contributed equally: Ana T. Pinto, Marta Pojo

Supplementary information The online version of this article (https://doi.org/10.1007/s12020-019-02009-5) contains supplementary material, which is available to authorized users.

✉ Branca M. Cavaco
bcavaco@ipolisboa.min-saude.pt

[1] Unidade de Investigação em Patobiologia Molecular (UIPM), Instituto Português de Oncologia de Lisboa Francisco Gentil (IPOLFG) E.P.E., Rua Prof. Lima Basto, 1099-023 Lisboa, Portugal

[2] Serviço de Endocrinologia, Instituto Português de Oncologia de Lisboa Francisco Gentil (IPOLFG) E.P.E., Rua Prof. Lima Basto, 1099-023 Lisboa, Portugal

[3] Faculdade de Ciências Médicas, Nova Medical School, Campo Mártires da Pátria 130, 1169-056 Lisboa, Portugal

[4] Serviço de Anatomia Patológica, Instituto Português de Oncologia de Lisboa Francisco Gentil (IPOLFG) E.P.E., Rua Prof. Lima Basto, 1099-023 Lisboa, Portugal

regional invasiveness makes it generally unresectable and resistant to chemotherapy/radiotherapy. The prognosis of ATC patients is very poor with a median survival of 5–6 months, with only 10–15% of ATC patients having 2 years of survival after diagnosis [2, 3]. These dedifferentiated tumors are characterized by many molecular alterations, namely, mutations in *BRAF*, *RAS*, *TERT* promoter, *TP53*, *PIK3CA*, *PTEN*, *CDKN2A*, and *CDKN2B* genes [4–6].

Presently, there is still a lack of truly effective therapies able to prolong patients' survival, being the current therapies only used as palliative care [7]. Therefore, there is an urgent need to better understand the biology of ATCs and develop new effective therapies. Human tumor-derived cell cultures are crucial tools in research, allowing to study cancer biology and predict drug resistance [8], avoiding the administration of ineffective chemotherapeutic drugs to patients. Several authors have successfully obtained ATC cell lines derived from surgically removed tumors [6, 9–12]. However, since the majority of ATCs are inoperable, fine-needle aspiration cytology (FNAC) has been considered as a good approach for obtaining primary ATC cell cultures [13].

Here we describe the establishment of a new ATC cell line (C3948), obtained from an unresectable ATC, through FNAC. A comprehensive genomic, cytogenetic, histopathological, and phenotypic (including drug resistance) characterization was performed. Our results show that C3948 retained the clinical features of the original cancer cells with respect to genetic and cytological alterations, presenting a drug-resistant profile similar to the commercial ATC cell line C643, and a unique gene expression and mutation profile. We therefore believe that this new cell line is a reliable model to investigate ATC biology, namely, new mutations and differentially expressed genes that could be responsible for drug resistance. This work supports the use of FNAC as a valuable strategy to obtain ATC cell cultures and to investigate the molecular mechanisms of ATC aggressiveness, which could help to predict tumor behavior and decide the best therapeutic strategy for each patient.

Materials and methods

Patient history

A 66-year-old male presented with a painful fast-growing neck mass for the past 2 months, associated with dysphonia and weight loss. Neck ultrasound revealed a tumor in the left lobe of thyroid gland with a thrombus in the internal jugular vein. Computed tomographic (CT) scan evidenced the same lesion, measuring 90 × 65 × 65 mm, pushing the trachea to the right, possibly infiltrating the paravertebral muscles, and mediastinal adenopathies, with the largest (76 × 18 mm) compressing the esophagus. The positron emission tomography-fluorodeoxyglucose/CT scan did not disclose additional metastatic foci. The initial classification of the tumor was IVB stage, according to American Joint Committe on Cancer Tumor, Metastasis, Node classification of malignant tumors [14]. A biopsy was obtained from the left cervical mass through FNAC, after approval by the institutional ethical review committee and patient's written informed consent. FNAC diagnosis was compatible with ATC. Owing to the unresectability of this lesion, the patient was submitted to cervical and mediastinal intensity-modulated radiation therapy (50 Gy in 25 fractions). However, the disease progressed under therapy, developing multiple pulmonary and pleural metastases and the patient died 6 months after the diagnosis.

Cell culture

Cells were cultured in RPMI-1640 medium with (C3948) or without (C643) Hepes (Gibco®, Life Technologies, Paisley, UK), supplemented with 1% L-Glutamine (Gibco®, Life Technologies, Paisley, UK), 1% Antibiotic–Antimycotic (Gibco®, Life Technologies, Paisley, UK), and 10% (v/v) fetal bovine serum (Merck Millipore, Berlin, Germany) and maintained at 37 °C and 5% CO_2. A short tandem repeat (STR) analysis was performed in C3948 (passages numbers 6 and 30) and C643 cells by STAB VIDA Genetics Lab. Mycoplasma-free culture was confirmed using the Universal Mycoplasma Detection Kit (ATCC, Manassas, VA, USA).

Hematoxylin and eosin (H&E) and immunohistochemistry

C3948 cells (collected at passage number 6) and FNAC specimen were immerged in 10% buffered formalin, to which hematoxylin was added. Cell blocks were prepared, using HistoGel™ (Thermo Scientific, Waltham, MA, USA, ref. HG-4000-012). After processing, the samples were sectioned and stained with H&E (Dako CoverStainer for H&E equipment, Agilent, Santa Clara, CA, USA). The protein expression of some epithelial and thyroid markers commonly used for thyroid cancer diagnosis was tested by immunocytochemistry using a BenchMark ULTRA Slide Staining System (Ventana, Oro Valley, AZ, USA) and CC1 standard antigen retrieval. The list of antibodies and respective conditions used are depicted in Supporting Table 1. Positive controls were included for all antibodies. OptiView (Ventana OptiView Kit, ref. 760-700) was used as a detection system. All samples were evaluated by a thyroid cancer expert pathologist.

Karyotype analysis

Karyotype analysis was performed as previously reported by Roque et al. [15]. In order to better identify the numerous

chromosomal markers observed, multicolor fluorescence in situ hybridization (M-FISH) using the 24×Cyte Human Multicolor FISH probe mix from MetaSystems (GmbH, Altussheim, Germany) was carried out as described by the manufacturer's instructions. Fluorochromes were sequentially captured in a Zeiss Imager Z1 microscope (Zeiss, Jena, Germany) linked to the M-FISH Cytovision software (Cytovision version 7.4, Leica Biosystems, Richmond, VA, USA). Twelve metaphases were collected and karyotypes were described according to ISCN (2016) [16].

Fluorescent in situ hybridization

For evaluation of *CDKN2A* gene copy number status of C3948 cells, a FISH analysis was applied to interphase nuclei using a commercial dual color probe (Vysis LSI CDKN2A SpectrumOrange/Vysis CEP 9 SpectrumGreen) (Abbott Molecular Inc., Des Plaines, IL, USA), according to the manufacturer's instructions. The LSI CDKN2A SpectrumOrange probe spans the 9p21 region that includes *CDKN2A* and *CDKN2B* genes, while the CEP 9 SpectrumGreen probe hybridizes to alpha satellite sequences specific to chromosome 9. FISH signals were captured and analyzed using a Zeiss epifluorescence microscope linked to a Cytovision FISH Probe software program (Cytovision version 7.4, Leica Biosystems, Richmond, VA, USA). Overlapping nuclei were excluded and individual and well-defined nuclei were analyzed. One hundred nuclei were scored and the number of orange (gene-specific) and green (chromosome-specific) signals were recorded.

DNA extraction

DNA was extracted from C3948 cells and ATC patient's peripheral blood using the Puregene^{R} Blood Core Kit (Qiagen, Hilden, Germany), following the manufacturer's protocol.

High resolution-comparative genomic hybridization (HR-CGH) analysis

HR-CGH from C3948 cell line was performed according to the method of Kallioniemi et al. [17], adapted as previously described [15]. For image analysis, a Zeiss epifluorescence microscope linked to a Cytovision HR-CGH software program (Cytovision version 7.4, Leica Biosystems, Richmond, VA, USA) was used. At least, 15 metaphases were acquired for the establishment of the HR-CGH profile.

Mutational analysis

DNA from C3948 cells was quantified with Qubit 2.0 Fluorometer (Invitrogen, Carlsbad, CA, USA) using the High Sensitivity DNA Kit (Invitrogen, Carlsbad, CA, USA). Fifty nanograms were analyzed by Next-Generation Sequencing (NGS) in a MiSeq sequencer platform (Illumina, San Diego, CA, USA), according to manufacturer's protocol. The commercial multigene panel (TruSight Cancer Panel, Illumina, San Diego, CA, USA) used was designed to target 94 genes (exons and splice site regions) associated with hereditary cancer predisposition, including the ATC-related genes *PTEN*, *TP53*, *CDKN2A* (p14^{ARF}, p16^{INK4A}), *CDKN1C* (p57), and *HRAS*. To exclude germline alterations in C3948, peripheral blood DNA from the respective ATC patient was also analyzed and only those alterations unique to the new established cell line were considered. Sequence data were analyzed on the instrument software MiSeq Reporter v.2.5.1 (Illumina), and the reads were aligned against the human reference sequence (hg19). The resulting VCF files were visualized using the Variant Studio Data Analysis v.2.2 software (Illumina). Bioinformatics analysis supplied the report of all detected sequence variants and the respective annotation. The following criteria were applied to select potentially relevant variants: (i) population frequency <1%, (ii) non-synonymous, (iii) total reads ≥5, and (iv) altered reads ≥3.

The entire coding sequence and exon–intron boundaries of several genes not included in NGS cancer panel but known to be important in thyroid tumorigenesis, such as those involved in the cell cycle [cyclin-dependent kinase inhibitors (CDKIs): *CDKN1A* (p21^{CIP1}), *CDKN1B* (p27^{KIP1}), and *CDKN2C* (p18^{INK4C})], were sequenced in C3948 cells, as previously described [6]. The sequence of a novel mutated thyroid cancer-related gene, *EIF1AX* (eukaryotic translation initiation factor 1A, X-linked) [18], was also analyzed as previously described [19]. The hotspot regions of *BRAF*, *NRAS*, *KRAS*, *PI3KCA*, and *TERT* promoter were also sequenced. The primer sequences and assay conditions are available in Supporting Table 2.

Microarray

Total RNA from C3948 and the commercial ATC cell line C643 was extracted and purified using the RNeasy Mini Kit (Qiagen, Hilden, Germany), according to the manufacturer's protocol. C643 cell line was authenticated, as previously described [20]. A pool of human thyroid total RNA obtained from 65 Caucasian individuals aged 18–61 years who died from sudden death (BD Bioscience, San Jose, CA, USA) was used as a control. After quantification by ultraviolet spectrophotometry (NanoDrop ND-1000, Thermo Fisher Scientific, Waltham, MA, USA) and integrity assessment by microcapillary electrophoresis (Agilent 2100 Bioanalyzer, Santa Clara, CA, USA), RNA was processed following the whole-transcript sense target labeling assay from Affymetrix and hybridized in a GeneChip™ Human Gene 2.1 ST Array (Affymetrix, Santa Clara, CA,

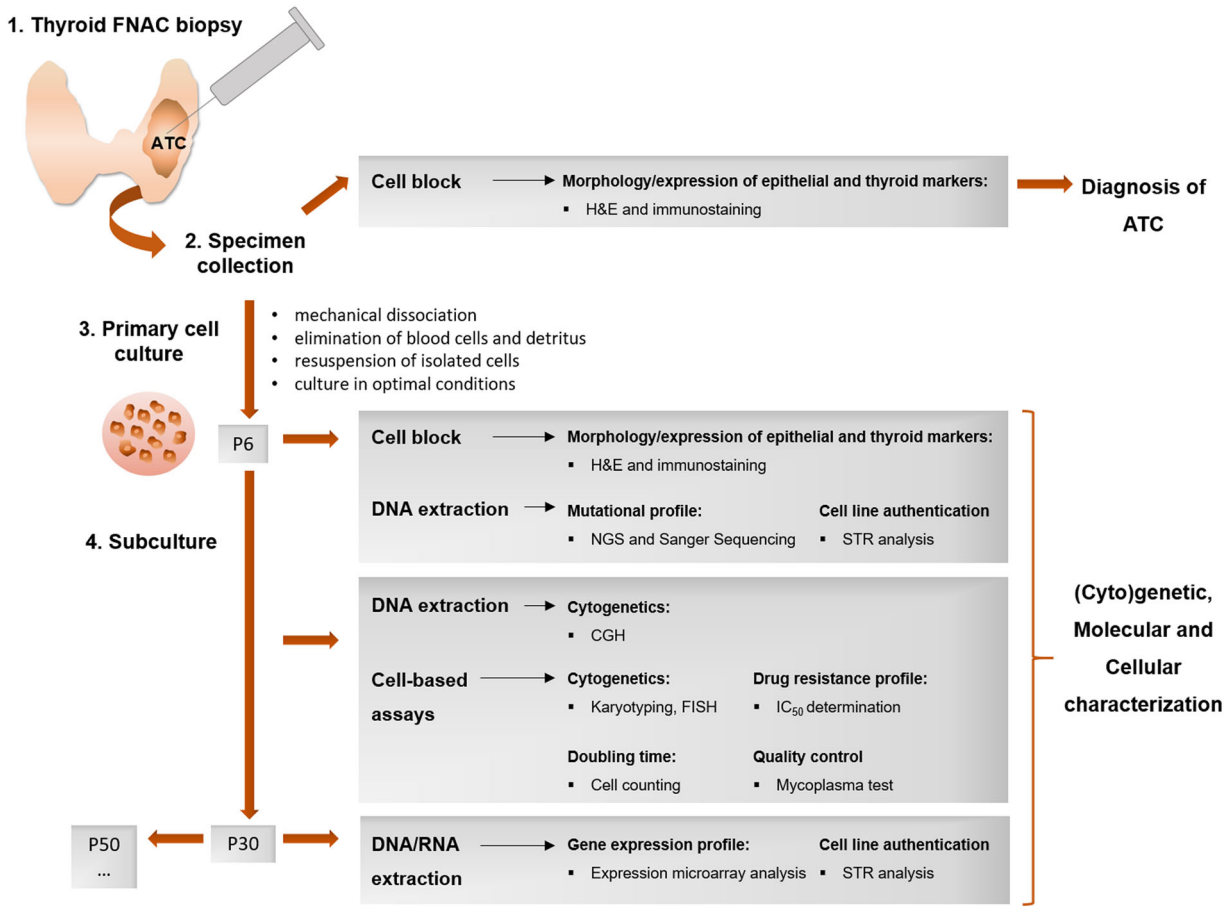

Fig. 1 Establishment of a new patient-derived ATC cell line - C3948. A thyroid cancer specimen was collected from a patient through FNAC. FNAC diagnosis was compatible with ATC. After mechanical dissociation of the cells within the specimen, elimination of blood cells and detritus and resuspension of isolated cells, a primary culture was obtained. This was subcultured for several passages to obtain a new patient-derived ATC cell line, which was characterized at (cyto) genetic, molecular and cellular levels. ATC anaplastic thyroid cancer, FNAC fine-needle aspiration cytology, CGH comparative genomic hybridization, NGS next-generation sequencing, H&E hematoxylin and eosin, P passage, STR short tandem repeat

USA). This array was designed with probes to measure both messenger (mRNA) and non-coding RNA. Microarray data analysis is presented in the Supporting information file.

IC_{50} determination

To determine the half-maximal inhibitory concentration (IC_{50}) of drugs commonly used in the treatment of ATCs, C3948 and C643 ATC cell lines were plated in 96-well plates (2×10^3 cells/well) and exposed to different concentrations of cisplatin (0.1, 0.5, 1, 2, 5, 8, 10, 15, and 20 µM), doxorubicin, and paclitaxel (0.05, 0.1, 0.2, 0.5, 1, 1.5, 2, 2.5, and 5 µM) for 72 h. Metabolic cell viability was determined by MTT [3-(4,5-dimethylthiazol-2-yl)-5-(3-carboxymethoxyphenyl)-2-(4-sulphophenyl)-2H-tetrazolium] (Promega, Madison, USA), at a final dilution of 1:20. IC_{50} values were calculated by a nonlinear regression (curve Fit) based on sigmoidal dose–response (variable slope) using GraphPad Prism 6.0 (GraphPad software, Inc., USA).

Doubling time calculation

For doubling time determination, C3948 and C643 ATC cell lines were plated in 6-well plates at an initial concentration of 60×10^3 cells/well. The cells were harvested with trypsin, stained with trypan blue, and the number of total viable cells was counted with a hemocytometer (0.100 mm, Neubauer Improved, Erlangen, Germany) at three time points after plating (24, 48, and 72 h). The cell doubling time was calculated using the Doubling Time software version 1.0.10 (http://www.doubling-time.com/compute.php).

Results

Establishment of a new ATC cell line

Cell aggregates from FNAC specimen were mechanically dissociated, blood cells and detritus were eliminated, and

isolated cells were resuspended in fresh medium (see "Materials and methods"). After 24 h, cells in suspension were plated into new wells, a procedure repeated for several days to increase the probability of obtaining more adherent cells. When confluent, cells were trypsinized and subcultured for >50 passages. An extensive characterization was performed at different cell passages (Fig. 1). The STR profile confirmed a consistent profile along culture time (Supporting Table 3)

C3948 has a histological phenotype representative of the original ATC cells

In order to confirm whether the new established cell line (C3948) maintained the same histological features as the original FNAC cells, we first compared the morphology of both samples. H&E staining of original ATC cells revealed the presence of cells with a marked pleomorphism, macronucleoli, fusocellular, and epithelioid morphology, with some multinucleated giant cells (Fig. 2a). A necrotic background with debris, macrophages and an inflammatory infiltrate was also observed, confirmed through an immunostaining for CD163, a macrophage marker (Fig. 2a). C3948 cells reproduced the morphology of the original ATC cells, with no aggregation, and with the absence of an inflammatory background indicating a clear isolation process free of contamination with other cell types (Fig. 2b).

In addition, both FNAC and C3948 cells were stained for epithelial (cytokeratin AE1/AE3, cytokeratin-19, and CAM5.2) and thyroid (thyroglobulin, calcitonin, and PAX-8 and TTF-1 transcription factors) markers, commonly used for thyroid cancer diagnosis. Results showed that both samples expressed AE1/AE3 and Cam5.2 but not cytokeratin 19 (Fig. 3a), thyroglobulin, calcitonin, PAX8, or TTF-1 (Fig. 3b). The histological features described are compatible with the diagnosis of undifferentiated/anaplastic carcinoma of the thyroid gland.

C3948 has a completely aberrant karyotype with many chromosomal losses and gains as the majority of ATCs

As previously reported for ATCs [21], C3948 cell culture also presented a very complex karyotype with clones with near triploid, near tetraploid, and near hexaploid chromosomal numbers (Fig. 4). The karyotype of the metaphase depicted in Fig. 4 is: 145 6n<138>XXY, der(X) t(X; 13; 19) x2, −X, −X −y,? der(y), 1, 1, 1, der(1) t(1;16)q?;?); der(1) t(1;19)(?;?); der (1) t(1;9)(?;?), 2, 2, 2, 2, −2, −2, 3, 3, der (3) t(3;2; 7;19)x2; der(3) t(3; 6; 13; 16;) der (3) t(X;3), 4, 4, 4, del (4)x3, ?4, 5, 5, 5, 5, 5, +del(5)(?q)x4, 6, 6, 6, 6, −6, −6, 7, 7, 7, 7, 7, 7, 7, 7, +del (7), +der (7) t(7; 19) 8, 8, 8, der (8) t(1;8), der (8) t (3, 7, 8, 13, 19), 9, 9, 9, 9, 9, 9, +del (9)x2; der(9) t (5;9), 10, 10, 10, 10, 10, 10, 10 11, 11, 11, 11, del (11) der (11) t(4; 10; 11), 12, 12, 12, 12, 12, −12, der (13) t (X; 2; 13; 19), der (13) t (8, 11, 13, 17, 22), der (13) (?dup13), der (13) t (X; 8; 13; 19; 21)x2, der (13) t (13;17) x2, (−14) x4, der (14) t(Y; 14; 20), 15, 15, 15, del (15q) x7, der(15) t(1; 15;20), +der(15) t(7; 15; 20), 16, 16, 16, 16, 16, der (16) (? dup16) x2, 17, 17, 17, 17, 17, 17, 18,

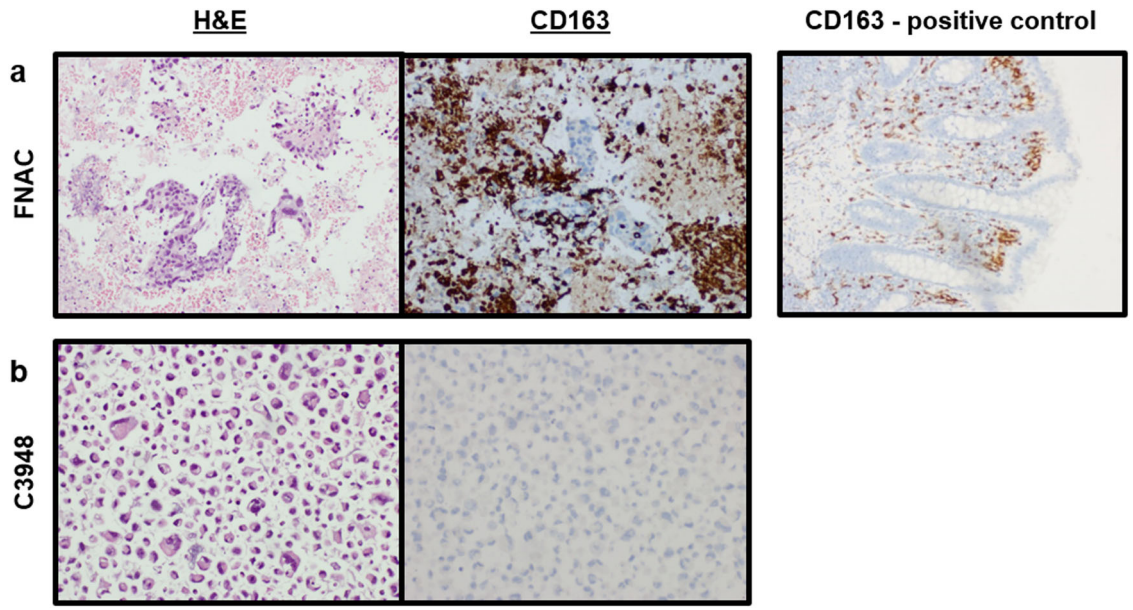

Fig. 2 Morphology and immune infiltration of fine-needle aspiration cytologic (FNAC) specimen and C3948 cell line. A hematoxylin and eosin staining revealed that **a** FNAC specimen had a marked pleomorphism, macronucleoli, fusocellular, and epithelioid morphology, with some multinucleated giant cells. **b** C3948 is representative of original cells but has no macrophage infiltration, as shown by CD163 staining

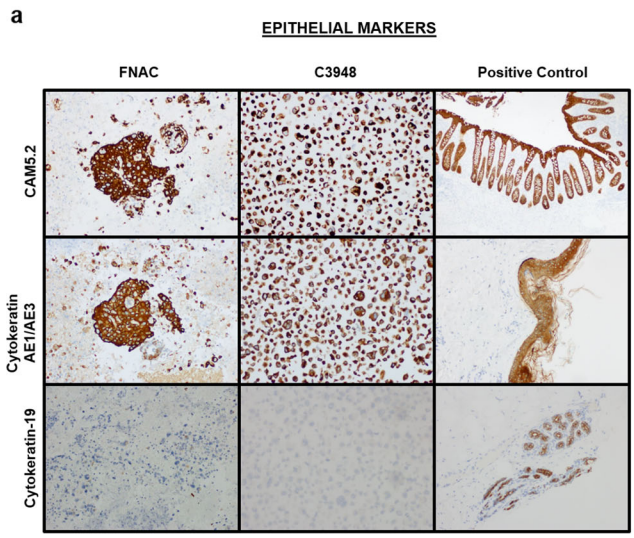

	Markers	FNAC	C3948
Epithelial	CAM5.2	+	+
	Cytokeratin AE1/AE3	+	+
	Cytokeratin 19	-	-

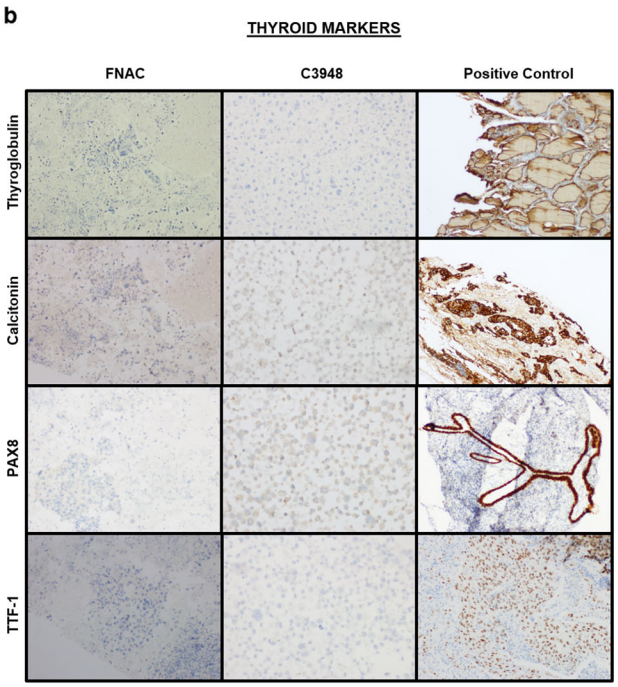

	Markers	FNAC	C3948
Thyroid	Thyroglobulin	-	-
	Calcitonin	-	-
	PAX8	-	-
	TTF-1	-	-

Fig. 3 Expression of epithelial and thyroid markers in the fine-needle aspiration cytologic (FNAC) specimen and C3948 cell line. Samples were stained for **a** epithelial and **b** markers commonly used for thyroid cancer diagnosis. Consistently, both FNAC and C3948 cells express CAM5.2 and cytokeratin AE1/AE3 but not cytokeratin-19, thyroglobulin, calcitonin, PAX-8, or TTF-1. All coverglasses were observed by an expert pathologist. + positive staining; − negative staining

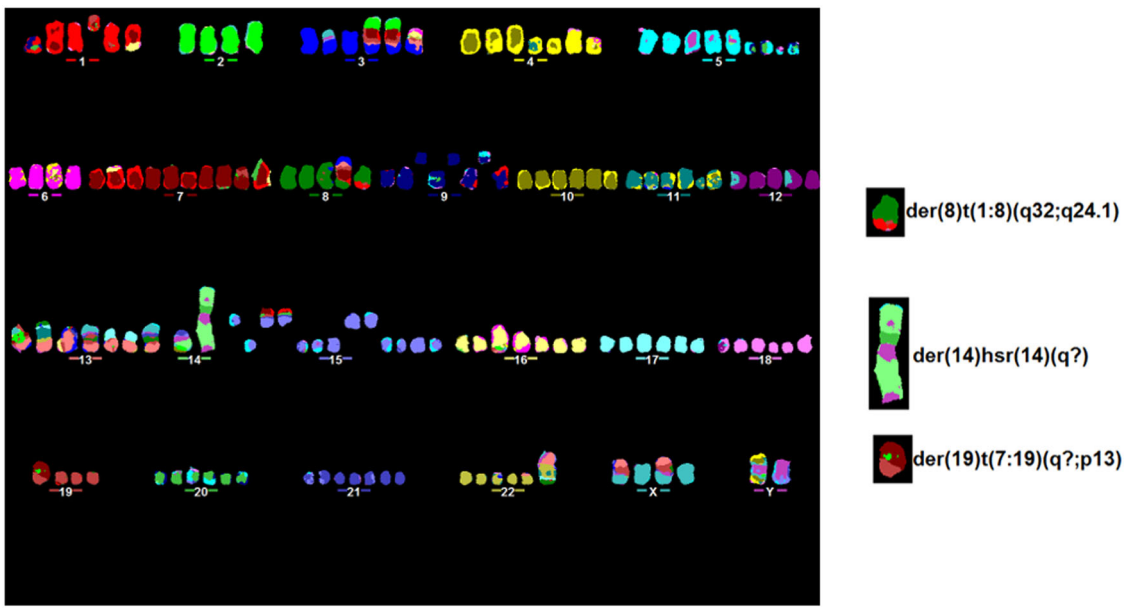

Fig. 4 Multicolor fluorescence in situ hybridization metaphase of C3948 cells. An aberrant karyotype with 145 chromosomes was observed

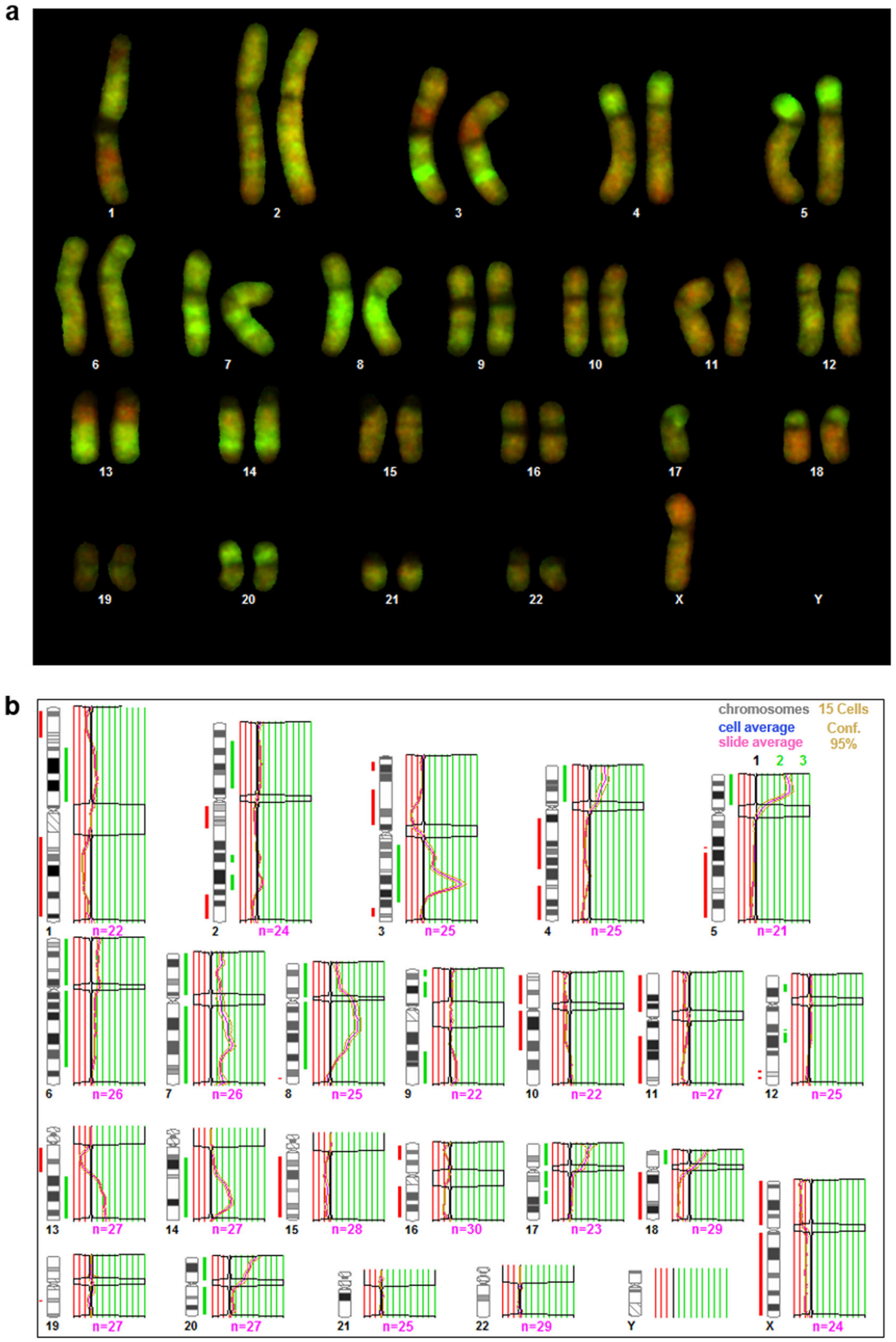

18, 18, del (18q) x2, der(18) t(12; 18), 19, 19, 19, −19, −19, +der(19)t(7;19), 20, 20, 20, 20, 20, 20, 21, 21, 21, 21, 21, 21, +21, 22, 22, 22, 22, 22, 22, der (22) t (8; 13, 22).

This cell line was characterized by an extensive genomic instability. None of the analyzed metaphases had a similar karyotype. Aberrations observed in 100% of the cells were:

◀ **Fig. 5** High-resolution comparative genomic hybridization (HR-CGH) analysis of C3948 cells. Images of **a** CGH karyotype and **b** CGH profile evidence many gains, amplifications, and losses of genetic material. The green (test DNA) to red (reference DNA) fluorescence ratio along the length of the chromosomes was calculated. This HR-CGH version uses dynamic standard reference intervals based on the systematic variation seen in normal samples. When the dynamic standard reference intervals do not overlap the confidence limits, the software interprets as either a loss (thresholds <0.75) or a gain (thresholds >1.25) in the test DNA. Thresholds >2.0 were considered to indicate high copy gains/amplifications. Heterochromatic regions in chromosomes 1, 9, 16, and Y and the p arms of the acrocentric chromosomes were discarded from the analysis

a del (5)(q?), a der (8) t(1;8)(q32; q24), a der (14) hsr(14)(q?), and a derivative chromosome 19 with a breakpoint at 19p13. The chromosomes rearranged with 19 were variable, being chromosome 7 the most frequently rearranged. Translocations involving chromosome 3 and X with two or more chromosomes were also observed in 100% of the metaphases. A detailed chromosomal analysis through HR-CGH showed a complex CGH profile with many gains, amplifications, and losses of genetic material, confirming the karyotype instability observed (Fig. 5; Supporting Table 4).

C3948 cells harbor mutated *TP53*, *STK11*, and *DIS3L2* genes

The DNA from both C3948 ATC cell line and matching ATC patient peripheral blood leukocytes were screened for mutations by NGS using a multigene panel. Three somatic genetic alterations were found, as they were detected exclusively in C3948 cells and not in patient's blood: c.1036G>T in *TP53*, c.647C>T in serine/threonine kinase 11 (*STK11*), and c.1082G>T in DIS3 like 3'-5' exoribonuclease 2 (*DIS3L2*) (Table 1). The assessment of intragenic polymorphisms in *TP53* revealed loss of heterozygosity in the tumor, which indicates that the variant was hemizygous. The variant in *TP53* is predicted to generate a truncated protein, while those in *STK11* and *DIS3L2* are missense variants. According to COSMIC database, the identified somatic variants in *STK11* and *TP53* were already reported in different carcinomas, namely, in lung adenocarcinoma. However, the variant found in *DIS3L2* is of unknown significance, being considered tolerated, possibly damaging or disease causing by different in silico prediction tools. Although cells in culture may acquire new features, the present molecular characterization was performed in DNA collected from a low passage after cell isolation.

In addition, a FISH analysis was performed to evaluate a possible biallelic deletion of *CDKN2A* ($p14^{ARF}$, $p16^{INK4A}$) suggested by NGS results. A commercial probe for 9p21 region, which covers the *CDKN2A/B* genes, and a probe control for the centromere of chromosome 9 were used. A

Table 1 Somatic variants detected by NGS in C3948 cells

Variant identification						In silico prediction		
Gene	Chr	Exon	Type	Nomenclature (HGVSc)	Predicted effect (HGVSp)	Sift	Polyphen	Mutation Taster
TP53[a]	17	10	Nonsense	c.1036G>T (NM_000546.5)	p.Glu346Ter (NP_000537.3)	–	–	Disease causing
STK11	19	5	Missense	c.647C>T (NM_000455.4)	p.Ser216Phe (NP_000446.1)	Deleterious (0)	Probably damaging (0.999)	Disease causing
DIS3L2	2	9	Missense	c.1082G>T (NM_152383.4)	p.Trp361Leu (NP_689596.4)	Tolerated (0.06)	Possibly damaging (0.553)	Disease causing

NGS next-generation sequencing

[a]HEM, hemizygosity is suggested by loss of heterozygosity at these *loci* in the tumor

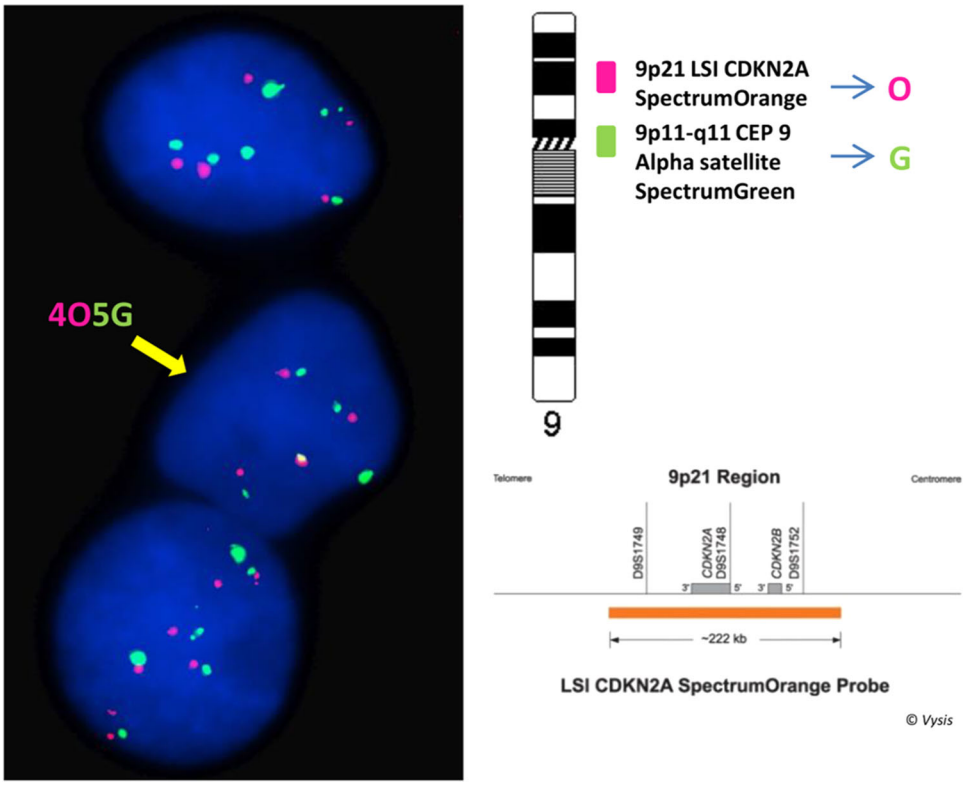

Fig. 6 Representative example of fluorescence in situ hybridization (FISH) analysis with the location and coverage of Vysis LSI. CDKN2A SpectrumOrange/Vysis CEP 9 SpectrumGreen Probes (adapted from Abbott) and image of FISH nuclei. The great variability of signal counts per nucleus is shown. In a normal cell, the expected pattern for nuclei hybridized with the LSI CDKN2A/ CEP 9 probe is the two Orange(O)/two-green signal (G) pattern (2 O/2 G), while a C3948 cell may have, e.g, a nucleus with four signals from the CDKN2A probe (4 O) and five signals from the centromere of chromosome 9 (5 G), as indicated by the arrow in the photo

great variability in signal counts per nuclei was observed: 56% of nuclei had gain of copies of both probes, e.g., with gains of 2, 3, and 4 copies in, respectively, 14, 20, and 8% of the nuclei scored; 42% nuclei had less copies of *CDKN2A* probe compared to the number of copies of the probe for the centromere of chromosome 9. As an example, 12% had 4 copies of *CDKN2A* probe and 5 copies of the centromere 9 (arrow in Fig. 6), and 12% had 5 copies of *CDKN2A* probe and 6 copies of centromere 9.

Other genes not included in NGS panel but important in thyroid tumorigeneses, such as those involved in cell cycle [CDKIs: *CDKN1A* ($p21^{CIP1}$), *CDKN1B* ($p27^{KIP1}$), and *CDKN2C* ($p18^{INK4C}$)] and a novel thyroid cancer-related gene (*EIF1AX*), were analyzed by Sanger sequencing, as well as hotspot regions of *BRAF*, *NRAS*, *KRAS*, *PI3KCA*, and *TERT* promoter. No alterations were found in any of these genes.

The gene expression profile of C3948 is similar to the C643 commercial ATC cell line when compared with normal thyroid tissue

We determined the global gene expression profile of both C3948 cells and the commercial ATC cell line C643 using RNA extracted from both cell lines and compared it with a commercial pool of normal human thyroid RNA. Hierarchical clustering of 31,135 transcripts showed that both ATC samples clustered together, separated from the normal thyroid pool sample (Fig. 7, Supporting Table 5).

Using a 2-fold change to define differentially expressed genes between ATC cell lines and normal thyroid, we obtained 1446 altered transcripts, including coding and non-coding RNAs, corresponding to 1391 genes (Fig. 8, Supporting Table 6). Almost 50% of them are deregulated in both ATC cell lines in comparison with normal thyroid tissue. Gene set enrichment analysis identified sets of commonly upregulated genes in both C3948 and C643 markedly related to *mitotic cell cycle*, while the downregulated ones are associated with *thyroid hormone metabolic process*.

Despite the similarity between the gene expression profiles of both ATC cell lines, >300 transcripts are exclusively deregulated in C3948 (Supporting Table 7). Gene enrichment analysis showed that upregulated IDs are associated with *DNA binding*, while the downregulated ones with the *reproductive system*.

The doubling time of both C3948 and C643 is similar

Doubling time during the exponential growth phase of C3948 was determined and compared with that of C643. The total number of viable cells was counted at 24, 48 and 72 h after plating (Fig. 9). Considering the exponential growth phase, the duplication time was of 30 h for C3948 and 23 h for C643. Although both cell lines presented a similar growth rate, that from C3948 was slightly lower than C643.

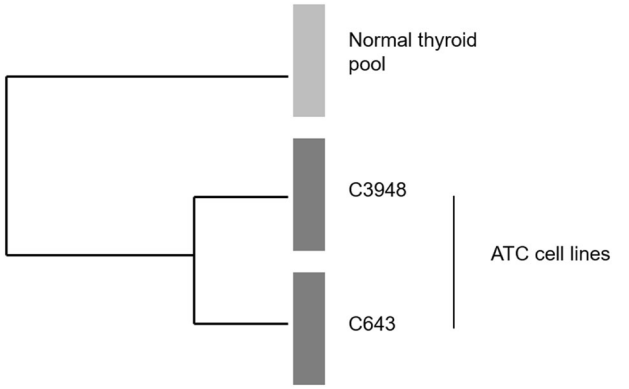

Fig. 7 Hierarchical clustering of a normal thyroid pool and C3948 and C643 anaplastic thyroid cancer (ATC) cell lines. Both ATC samples clustered together, separated from the normal one. Distance separating samples represents the gene expression resemblance between them. Analysis was performed using the GeneCluster and TreeView software

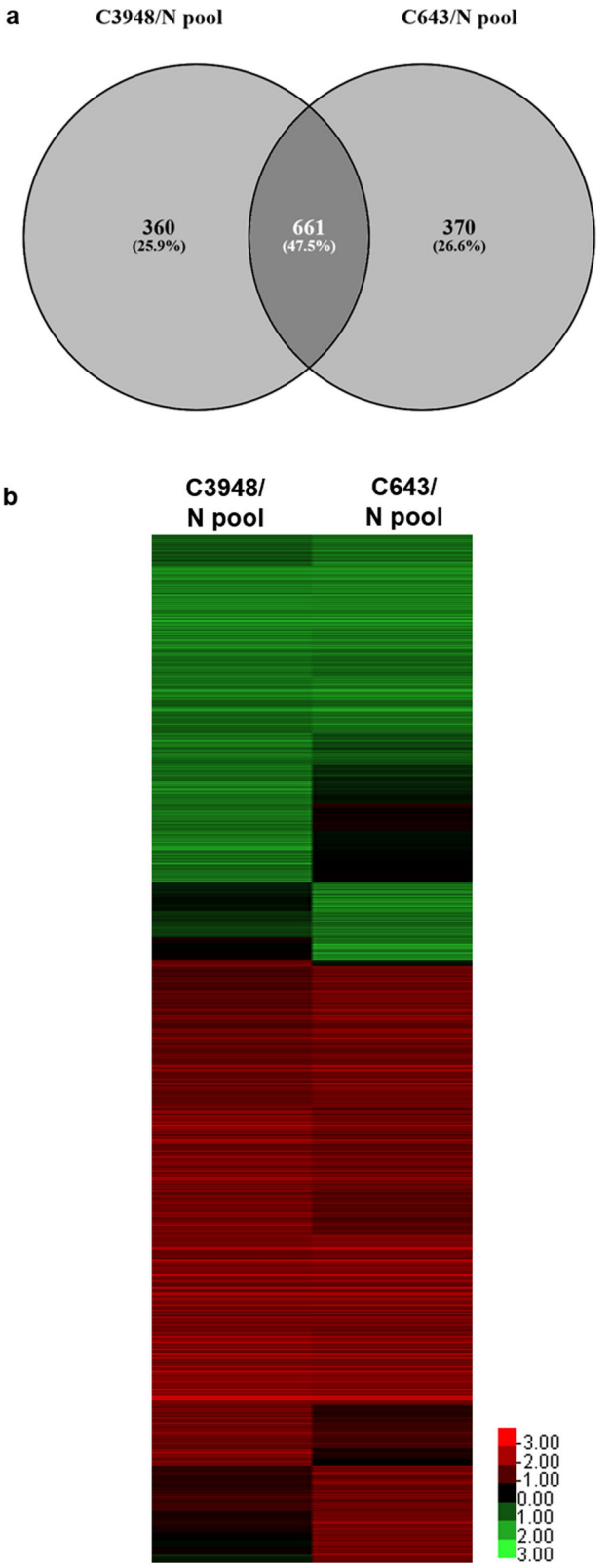

The IC50 profile for paclitaxel, doxorubicin, and cisplatin is similar in both C643 and C3948, although higher for cisplatin in C3948

We determined the half maximal inhibitory concentration (IC_{50}) of three anticancer agents (doxorubicin, cisplatin, and paclitaxel) commonly used in ATC palliative care (Fig. 10). The graph evidences a similar IC_{50} profile within the same range of values for each of the three drugs tested in both C3948 and C643, with cisplatin presenting the highest IC_{50} value and paclitaxel the lowest one, indicating that paclitaxel was the most efficient drug evaluated. Considering the IC_{50} value of cisplatin in each cell line (5.7 μM ± 0.66 for C643 and 12.1 μM ± 3.43 for C3948), this drug induced a significantly higher decrease in C643 viability than in C3948 cells.

Discussion

ATCs are very aggressive tumors, often inoperable, with no current effective treatments. As validated by Antonelli and colleagues [13], FNAC is an essential methodology to access this biological material and establish patient-derived ATC cell lines to further study ATC drug resistance.

In the present work, ATC cells were collected through FNAC to establish a new patient-derived cancer cell line (C3948), which was further characterized. The fidelity of C3948 to the characteristics of the originating tumor was first checked, as an essential validation step that should be done when isolating ATC cells from patients [11, 22]. Immunostaining showed that, similar to the original ATC cells, C3948 expressed CAM5.2 and cytokeratin AE1/AE3 epithelial markers but not cytokeratin 19 or thyroid-related markers (thyroglobulin and calcitonin) or transcription factors (PAX-8, TTF-1).

◀ **Fig. 8** Gene expression profile of C3948 and C643 anaplastic thyroid cancer (ATC) cell lines, compared with a normal thyroid pool. **a** A Venn diagram represents the number of differentially expressed genes shared between C3948 and C643, when compared to normal thyroid tissue. **b** A heat map evidences the 1446 transcripts differentially expressed between ATC cell lines (C3948 and/or C643) and normal thyroid tissue. Data are presented in logarithmic scale, with light red color evidencing the most downregulated genes and light green color the most upregulated ones

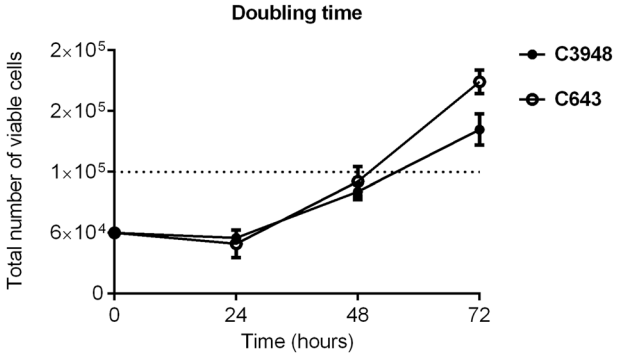

Fig. 9 Doubling time analysis in C3948 and C643 anaplastic thyroid cancer cell lines. MTT (3-(4,5-dimethylthiazol-2-yl)-5-(3-carboxymethoxyphenyl)-2-(4-sulphophenyl)-2H-tetrazolium) assay revealed that C3948 presents a slightly lower doubling time than C643. The total number of cells represent the mean and standard deviation of at least three independent experiments

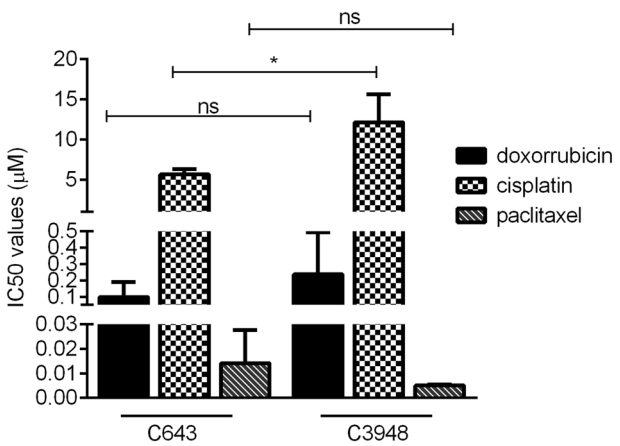

Fig. 10 IC_{50} values for doxorubicin, cisplatin, and paclitaxel in C643 and C3948 anaplastic thyroid cancer cell lines. A similar profile was found for both cell lines, although IC_{50} of cisplatin is higher for C3948. The IC_{50} values represent the mean and standard deviation of at least three independent experiments. ns, non-significant. *$p < 0.05$

ATCs commonly present a highly complex genome with multiple breakpoints and large variation in copy numbers [23]. Accordingly, C3948 cells present an aberrant karyotype with many losses and gains of genetic material. Regarding their mutational landscape, ATCs are a highly heterogeneous group of tumors and distinct percentages of the same mutated genes are observed in different published cohorts [4–6], making difficult to define a unique panel of altered genes in ATC. However, it is assumed that the majority of ATCs harbor mutations in *TP53* tumor-suppressor gene, which may confer them an aggressive phenotype [24]. Frequent mutations can also be found in *HRAS/KRAS/NRAS*, *CDKIs*, *TERT* promoter, *PTEN*, *PIK3CA*, or *EIF1AX* [4–6, 25–27]. The commercial ATC cell line C643, which we used for comparison, also harbors mutated *TP53* and *HRAS* [6]. Besides *TP53*, C3948 also presents genetic alterations in other tumor-suppressor genes, such as *STK11* [serine/threonine kinase 11, also known as Liver Kinase B1 (*LKB1*)] and *DIS3L2*.

STK11 is involved in cellular responses such as energy metabolism, cell polarity and cell growth and, when catalytically active, is able to phosphorylate 14 serine/threonine kinases of the AMPK family [28]. In a mouse model, *STK11* was found to suppress lung tumorigenesis, influencing tumor initiation, differentiation, and metastasis [29]. Somatic mutations in *STK11*, although rare, have been reported in different types of cancer, namely cervix, colorectal, and lung cancers [30] (COSMIC database v88, released 19-MAR-19). The co-existence of mutations in *STK11* and *TP53* in ATC samples as we reported were also previously found by Landa and colleagues [4], although at a low frequency (6%) and associated with mutations in *NRAS* or *PI3K/AKT/SWISNF/MMR*. Particularly the *STK11* missense variant (C.647C>T) described in our work was also detected in human lung adenocarcinoma cells [29]. This mutation is located in exon 5 and involves the functional domain VIII of the protein [31], being expected to impair STK11 kinase activity, since domain VIII, together with domains VIB and VII, is a site of substrate recognition and phosphate transfer initiation [31].

C3948 cells also harbor a missense variant in *DIS3L2* gene (c.1082G>T) never described before. *DIS3L2* is a 3'-5' exonuclease that degrades uridylated miRNAs, namely, let-7 precursor RNAs, the expression of which is blocked by the RNA-binding proteins Lin28A and Lin28B [32]. Interestingly, according to our microarray data, and when compared with normal thyroid tissue, *LIN28* mRNA expression is upregulated in C3948 but not in C643 (Supporting Table 5).

In summary, we report the establishment of a new ATC cell line obtained from a FNAC, designated as C3948, which is representative of the original cells. Comparison of the genetic profiles of this cell line and that of the commercial ATC cell line C643 evidenced the similarity between them and emphasizes C3948 as a new ATC cell line. Despite similarities, C3948 has also some unique features, such as additional mutations in *STK11* and *DIS3L2* genes which, together with an aberrant karyotype, may have contributed to disease progression. Therefore, it seems relevant to perform in vitro tests to further explore the role of these genetic variants in ATC aggressiveness and drug

resistance. ATCs are very heterogeneous and it remains crucial to identify the unique mutation profile associated with each ATC patient. To achieve that, the analysis of multigene panels by NGS is already used in many centers for cancer diagnosis, prognosis, and therapeutic selection/response, and feasibility studies have demonstrated its clinical utility, showing that a focused panel may be sufficient to detect major mutations [33, 34].

Acknowledgements The authors are thankful for the collaboration of the Endocrinology (Dr. Rita Santos) and Pathology Departments from Instituto Português de Oncologia de Lisboa Francisco Gentil (IPOLFG). This work was funded by Associação de Endocrinologia Oncológica (AEO), IPOLFG and iNOVA4Health Research Unit (LISBOA-01-0145-FEDER-007344), which is cofunded by Fundação para a Ciência e Tecnologia/Ministério da Ciência e do Ensino Superior, through national funds, and by FEDER under the PT2020 Partnership Agreement. M.P. was supported by Núcleo Regional Sul da Liga Portuguesa Contra o Cancro.

Compliance with ethical standards

Conflict of interest The authors declare that they have no conflict of interest.

Ethical approval All procedures performed in studies involving human participants were in accordance with the ethical standards of the institutional and/or national research committee and with the 1964 Helsinki declaration and its later amendments or comparable ethical standards.

Informed consent Informed consent was obtained from all individual participants included in the study.

Publisher's note: Springer Nature remains neutral with regard to jurisdictional claims in published maps and institutional affiliations.

References

1. M. Ragazzi, A. Ciarrocchi, V. Sancisi, G. Gandolfi, A. Bisagni, S. Piana, Update on anaplastic thyroid carcinoma: morphological, molecular, and genetic features of the most aggressive thyroid cancer. Int. J. Endocrinol. **2014**, 790834 (2014). https://doi.org/10.1155/2014/790834
2. E. Kebebew, F.S. Greenspan, O.H. Clark, K.A. Woeber, A. McMillan, Anaplastic thyroid carcinoma. Treatment outcome and prognostic factors. Cancer **103**, 1330–1335 (2005). https://doi.org/10.1002/cncr.20936
3. R.C. Smallridge, L.A. Marlow, J.A. Copland, Anaplastic thyroid cancer: molecular pathogenesis and emerging therapies. Endocr. Relat. Cancer **16**, 17–44 (2009). https://doi.org/10.1677/ERC-08-0154
4. I. Landa, T. Ibrahimpasic, L. Boucai, R. Sinha, J.A. Knauf, R.H. Shah, S. Dogan, J.C. Ricarte-Filho, G.P. Krishnamoorthy, B. Xu, N. Schultz, M.F. Berger, C. Sander, B.S. Taylor, R. Ghossein, I. Ganly, J.A. Fagin, Genomic and transcriptomic hallmarks of poorly differentiated and anaplastic thyroid cancers. J. Clin. Invest. **126**, 1052–1066 (2016). https://doi.org/10.1172/JCI85271
5. J.W. Kunstman, C.C. Juhlin, G. Goh, T.C. Brown, A. Stenman, J. M. Healy, J.C. Rubinstein, M. Choi, N. Kiss, C. Nelson-Williams, S. Mane, D.L. Rimm, M.L. Prasad, A. Hoog, J. Zedenius, C. Larsson, R. Korah, R.P. Lifton, T. Carling, Characterization of the mutational landscape of anaplastic thyroid cancer via whole-exome sequencing. Hum. Mol. Genet. **24**, 2318–2329 (2015). https://doi.org/10.1093/hmg/ddu749
6. J.M. Pita, I.F. Figueiredo, M.M. Moura, V. Leite, B.M. Cavaco, Cell cycle deregulation and TP53 and RAS mutations are major events in poorly differentiated and undifferentiated thyroid carcinomas. J. Clin. Endocrinol. Metab. **99**, E497–E507 (2014). https://doi.org/10.1210/jc.2013-1512
7. R.C. Smallridge, K.B. Ain, S.L. Asa, K.C. Bible, J.D. Brierley, K. D. Burman, E. Kebebew, N.Y. Lee, Y.E. Nikiforov, M.S. Rosenthal, M.H. Shah, A.R. Shaha, R.M. Tuttle, American Thyroid Association Anaplastic Thyroid Cancer Guidelines Taskforce, American Thyroid Association guidelines for management of patients with anaplastic thyroid cancer. Thyroid **22**, 1104–1139 (2012). https://doi.org/10.1089/thy.2012.0302
8. S.V. Sharma, D.A. Haber, J. Settleman, Cell line-based platforms to evaluate the therapeutic efficacy of candidate anticancer agents. Nat. Rev. Cancer **10**, 241–253 (2010). https://doi.org/10.1038/nrc2820
9. H. Asakawa, T. Kobayashi, Y. Komoike, T. Yanagawa, M. Takahashi, E. Wakasugi, H. Maruyama, Y. Tamaki, Y. Matsuzawa, M. Monden, Establishment of anaplastic thyroid carcinoma cell lines useful for analysis of chemosensitivity and carcinogenesis. J. Clin. Endocrinol. Metab. **81**, 3547–3552 (1996). https://doi.org/10.1210/jcem.81.10.8855799
10. M. Garg, R. Okamoto, Y. Nagata, D. Kanojia, S. Venkatesan, M. T.A., G.D. Braunstein, J.W. Said, N.B. Doan, Q. Ho, T. Akagi, S. Gery, L.Z. Liu, K.T. Tan, W.J. Chng, H. Yang, S. Ogawa, H.P. Koeffler, Establishment and characterization of novel human primary and metastatic anaplastic thyroid cancer cell lines and their genomic evolution over a year as a primagraft. J. Clin. Endocrinol. Metab. **100**, 725–735 (2015). https://doi.org/10.1210/jc.2014-2359
11. N. Onoda, M. Nakamura, N. Aomatsu, S. Noda, S. Kashiwagi, K. Hirakawa, Establishment, characterization and comparison of seven authentic anaplastic thyroid cancer cell lines retaining clinical features of the original tumors. World J. Surg. **38**, 688–695 (2014). https://doi.org/10.1007/s00268-013-2409-7
12. F. Stenner, H. Liewen, M. Zweifel, A. Weber, J. Tchinda, B. Bode, P. Samaras, S. Bauer, A. Knuth, C. Renner, Targeted therapeutic approach for an anaplastic thyroid cancer in vitro and in vivo. Cancer Sci. **99**, 1847–1852 (2008). https://doi.org/10.1111/j.1349-7006.2008.00882.x
13. A. Antonelli, S.M. Ferrari, P. Fallahi, P. Berti, G. Materazzi, I. Marchetti, C. Ugolini, F. Basolo, P. Miccoli, E. Ferrannini, Evaluation of the sensitivity to chemotherapeutics or thiazolidinediones of primary anaplastic thyroid cancer cells obtained by fine-needle aspiration. Eur. J. Endocrinol. **159**, 283–291 (2008). https://doi.org/10.1530/EJE-08-0190
14. J.D. Brierley, M.K. Gospodarowicz, C. Wittekind, *TNM Classification of Malignant Tumours*, 8th edn. (Wiley, Hoboken, NJ, 2017)
15. L. Roque, R. Rodrigues, A. Pinto, V. Moura-Nunes, J. Soares, Chromosome imbalances in thyroid follicular neoplasms: a comparison between follicular adenomas and carcinomas. Genes Chromosomes Cancer **36**, 292–302 (2003). https://doi.org/10.1002/gcc.10146
16. J. McGowan-Jordan, A. Simons, M. Schmid, *ISCN 2016: An International System for Human Cytogenomic Nomenclature*, vol. 149, 1st edn. Reprint of *Cytogenetic and Genome Research* (Karger, Basel, 2016)
17. O.P. Kallioniemi, A. Kallioniemi, J. Piper, J. Isola, F.M. Waldman, J.W. Gray, D. Pinkel, Optimizing comparative genomic hybridization for analysis of DNA sequence copy number changes in solid tumors. Genes Chromosomes Cancer **10**, 231–243 (1994)

18. N. Cancer Genome Atlas Research, Integrated genomic characterization of papillary thyroid carcinoma. Cell **159**, 676–690 (2014). https://doi.org/10.1016/j.cell.2014.09.050
19. J. Simoes-Pereira, M.M. Moura, I.J. Marques, M. Rito, R.A. Cabrera, V. Leite, B.M. Cavaco, The role of EIF1AX in thyroid cancer tumourigenesis and progression. J. Endocrinol. Invest. (2018). https://doi.org/10.1007/s40618-018-0919-8
20. S. Lopes-Ventura, M. Pojo, A.T. Matias, M.M. Moura, I.J. Marques, V. Leite, B.M. Cavaco, The efficacy of HRAS and CDK4/6 inhibitors in anaplastic thyroid cancer cell lines. J. Endocrinol. Invest. (2018). https://doi.org/10.1007/s40618-018-0947-4
21. R.F. Rodrigues, L. Roque, T. Krug, V. Leite, Poorly differentiated and anaplastic thyroid carcinomas: chromosomal and oligo-array profile of five new cell lines. Br. J. Cancer **96**, 1237–1245 (2007). https://doi.org/10.1038/sj.bjc.6603578
22. L.A. Marlow, J. D'Innocenzi, Y. Zhang, S.D. Rohl, S.J. Cooper, T. Sebo, C. Grant, B. McIver, J.L. Kasperbauer, J.T. Wadsworth, J.D. Casler, P.W. Kennedy, W.E. Highsmith, O. Clark, D. Milosevic, B. Netzel, K. Cradic, S. Arora, C. Beaudry, S.K. Grebe, M. L. Silverberg, D.O. Azorsa, R.C. Smallridge, J.A. Copland, Detailed molecular fingerprinting of four new anaplastic thyroid carcinoma cell lines and their use for verification of RhoB as a molecular therapeutic target. J. Clin. Endocrinol. Metab. **95**, 5338–5347 (2010). https://doi.org/10.1210/jc.2010-1421
23. E.L. Woodward, A. Biloglav, N. Ravi, M. Yang, L. Ekblad, J. Wennerberg, K. Paulsson, Genomic complexity and targeted genes in anaplastic thyroid cancer cell lines. Endocr. Relat. Cancer **24**, X2 (2017). https://doi.org/10.1530/ERC-16-0522e
24. J.A. Fagin, K. Matsuo, A. Karmakar, D.L. Chen, S.H. Tang, H.P. Koeffler, High prevalence of mutations of the p53 gene in poorly differentiated human thyroid carcinomas. J. Clin. Invest. **91**, 179–184 (1993). https://doi.org/10.1172/JCI116168
25. M. Xing, Molecular pathogenesis and mechanisms of thyroid cancer. Nat. Rev. Cancer **13**, 184–199 (2013). https://doi.org/10.1038/nrc3431
26. N. Pozdeyev, L.M. Gay, E.S. Sokol, R. Hartmaier, K.E. Deaver, S. Davis, J.D. French, P.V. Borre, D.V. LaBarbera, A.C. Tan, R. E. Schweppe, L. Fishbein, J.S. Ross, B.R. Haugen, D.W. Bowles, Genetic analysis of 779 advanced differentiated and anaplastic thyroid cancers. Clin. Cancer Res. **24**, 3059–3068 (2018). https://doi.org/10.1158/1078-0432.CCR-18-0373
27. I. Landa, N. Pozdeyev, C. Korch, L.A. Marlow, R.C. Smallridge, J.A. Copland, Y.C. Henderson, S.Y. Lai, G.L. Clayman, N. Onoda, A.C. Tan, M.E.R. Garcia-Rendueles, J.A. Knauf, B.R. Haugen, J.A. Fagin, R.E. Schweppe, Comprehensive genetic characterization of human thyroid cancer cell lines: a validated panel for preclinical studies. Clin. Cancer Res. (2019). https://doi.org/10.1158/1078-0432.CCR-18-2953
28. S.E. Korsse, M.P. Peppelenbosch, W. van Veelen, Targeting LKB1 signaling in cancer. Biochim. Biophys. Acta **1835**, 194–210 (2013). https://doi.org/10.1016/j.bbcan.2012.12.006
29. H. Ji, M.R. Ramsey, D.N. Hayes, C. Fan, K. McNamara, P. Kozlowski, C. Torrice, M.C. Wu, T. Shimamura, S.A. Perera, M. C. Liang, D. Cai, G.N. Naumov, L. Bao, C.M. Contreras, D. Li, L. Chen, J. Krishnamurthy, J. Koivunen, L.R. Chirieac, R.F. Padera, R.T. Bronson, N.I. Lindeman, D.C. Christiani, X. Lin, G.I. Shapiro, P.A. Janne, B.E. Johnson, M. Meyerson, D.J. Kwiatkowski, D.H. Castrillon, N. Bardeesy, N.E. Sharpless, K.K. Wong, LKB1 modulates lung cancer differentiation and metastasis. Nature **448**, 807–810 (2007). https://doi.org/10.1038/nature06030
30. V. Launonen, Mutations in the human LKB1/STK11 gene. Hum. Mutat. **26**, 291–297 (2005). https://doi.org/10.1002/humu.20222
31. N. Hearle, V. Schumacher, F.H. Menko, S. Olschwang, L.A. Boardman, J.J. Gille, J.J. Keller, A.M. Westerman, R.J. Scott, W. Lim, J.D. Trimbath, F.M. Giardiello, S.B. Gruber, G.J. Offerhaus, F.W. de Rooij, J.H. Wilson, A. Hansmann, G. Moslein, B. Royer-Pokora, T. Vogel, R.K. Phillips, A.D. Spigelman, R.S. Houlston, Frequency and spectrum of cancers in the Peutz-Jeghers syndrome. Clin. Cancer Res. **12**, 3209–3215 (2006). https://doi.org/10.1158/1078-0432.CCR-06-0083
32. H.M. Chang, R. Triboulet, J.E. Thornton, R.I. Gregory, A role for the Perlman syndrome exonuclease Dis3l2 in the Lin28-let-7 pathway. Nature **497**, 244–248 (2013). https://doi.org/10.1038/nature12119
33. Y. Naito, H. Takahashi, K. Shitara, W. Okamoto, H. Bando, T. Kuwata, Y. Kuboki, S. Matsumoto, I. Miki, T. Yamanaka, A. Watanabe, M. Kojima, Feasibility study of cancer genome alterations identified by next generation sequencing: ABC study. Jpn. J. Clin. Oncol. **48**, 559–564 (2018). https://doi.org/10.1093/jjco/hyy052
34. G. Zheng, H. Tsai, L.H. Tseng, P. Illei, C.D. Gocke, J.R. Eshleman, G. Netto, M.T. Lin, Test feasibility of next-generation sequencing assays in clinical mutation detection of small biopsy and fine needle aspiration specimens. Am. J. Clin. Pathol. **145**, 696–702 (2016). https://doi.org/10.1093/ajcp/aqw043